Mechanism of a disassembly-driven sensing system studied by stopped-flow kinetics

Gallo, C., Thomas, S. S., Selinger, A. J., Hof, F., & Bohne, C.

2021

The final publication is available via ACS Publications at:

https://doi.org/10.1021/acs.joc.1c00959

Mechanism of a Disassembly Driven Sensing System Studied by Stopped-Flow Kinetics

Cara Gallo, Suma S. Thomas, Allison J. Selinger, Fraser Hof* and Cornelia Bohne*

Department of Chemistry and Centre for Advanced Materials and Related Technologies (CAMTEC), University of Victoria, PO Box 1700 STN CSC, Victoria, BC V8W 2Y2, Canada

Supporting Information Placeholder

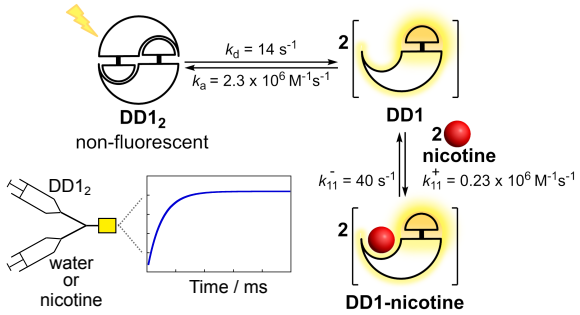

ABSTRACT: We carried out steady-state and stopped-flow photophysical measurements to determine the kinetics of a discrete disassembly driven turn-on fluorescent system. On and off rates for both DimerDye1 (DD1) assembly, and nicotine binding were determined. Relative rates for these competing processes provide insight on how this system can be optimized for sensing applications. Kinetics studies in artificial saliva showed that moving to more complex media has minimal effects on the sensing ability of the system.

In supramolecular sensing, the coupling of a molecular recognition event to a fluorescent output can happen in many ways.[1-5] Analyte-triggered disaggregation is a broadly successful approach for turn-on fluorescence sensing.[6-8] Amphiphilic dendrimers and polymers — easily functionalized and intrinsically suited to forming large aggregates — are often used for disassembly-driven sensing.[9-13] Host-guest binding can also be used to trigger the disassembly of molecular micelles, in order to provide visible responses. Where a host-indicator complex forms large, quenched micellar aggregates, the presence of a guest-type analyte can cause disassembly and render the indicator emissive.[14] This approach is operational in complex biological and aqueous media, and has been used as a general approach for selectively sensing drugs,[15-16] and biologically relevant analytes.[17-19]

Mechanistic details about dynamic phenomena are germane for the design of complex systems at equilibrium or out-of-equilbrium.[5, 20-22] Studies for tandem assays based on host-guest disassembly showed that disassembly must be faster than the assayed reaction.[23] The micellar or polymeric nature of many disassembly-driven sensors complicates their mechanistic characterization.[24] In contrast, knowledge on how to control sequential and competitive pathways for stoichiometric disassembly systems will provide the information required for the optimization of such systems.

Scheme 1. Fluorescence turn-on of the HSP moiety of DD1 with the binding of nicotine guest.

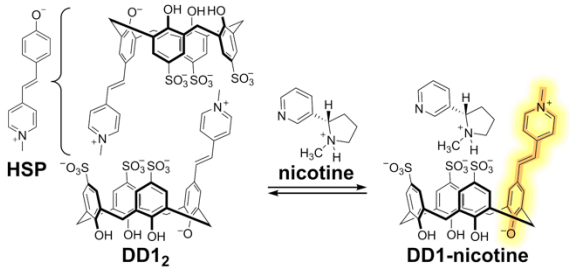

We have previously reported a series of calixarenes that homodimerize in water.[25] Analogs that include an integrated fluorescent component are called DimerDyes.[26-27] The self-assembly of DimerDyes stacks two dye copies in an antiparallel, quenching arrangement. The addition of a good guest out-competes homodimerization to form a host-guest complex, resulting in a turn-on fluorescence response (Scheme 1). These disassembly-driven systems are inherently resistant to interference from

competing co-solutes,[28] making them well suited to many biosensing tasks. As discrete assemblies, DimerDyes are uniquely well suited to detailed mechanistic characterization.

The current study focuses on the competing binding equilibria for the complexes of DimerDye1 (DD1) with the guest nicotine. Nicotine is a biologically relevant model analyte[27, 29] that has multiple ionizable groups ($pK_a = 3.1$ (pyridine) and 8.0 (pyrrolidine)),[30] allowing us to probe the effect of charge on multiple binding equilibria. We first characterize the general assembly and photophysical properties of the system using absorbance and steady-state fluorescence. We then used stopped-flow experiments in buffer and artificial saliva to establish the kinetics of individual steps, and to reveal how complex media affect the kinetics at the heart of this disassembly-driven sensor.[31]

Dimerization of DD1 is affected by the protonation states of the host. Sulfonatocalix[4]arenes have a single, unusually acidic phenol with a pK_a of 3.2, while the remaining three phenols have pK_a values ≥11.3.[32-33] At pH 6.3 (one anionic phenol, Scheme 1) and at pH 12.1 (>1 anionic phenol) DD1 exists as the non-fluorescent dimeric $DD1_2$ (inset Figure 1a,b).[26] At pH 2.2, some fluorescence is observed (Figure 1b), indicating the presence of the fluorescent monomer DD1. This weakening of the dimer is likely due to the pH being lower than the pK_a of the hydroxyl group on the lower rim of DD1.

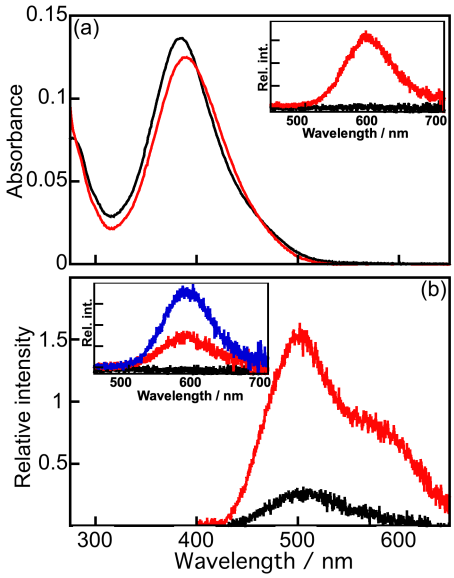

Figure 1. (a) Absorption and fluorescence (inset) spectra for 8.3 μM DD1 in the absence (black) and presence (red) of 167 μM nicotine at pH 6.3. (b) Fluorescence spectra for 8.3 μM DD1 in the absence (black) and presence of 167 μM nicotine (red) at pH 2.2. Inset: Fluorescence spectra for 10 μM DD1 in the absence (black) and presence of 500 (red) and 2000 μM (blue) choline at pH 12.1.

Optimal DD1-guest binding occurs with positively charged guests. Upon treatment with nicotine at pH 6.3 and 2.2, a red shift in the absorption spectra and increase in emission intensities are observed (Figure 1, S1). This is expected to arise from the disassembly of $DD1_2$ and formation of the DD1-nicotine complex. The existence of some disassembled DD1 at pH 2.2 leads to detectable fluorescence in the absence of nicotine, which signifies the presence of a mixture of species. At pH 12.1, nicotine is uncharged; the minimal response of DD1 absorbance and emission upon addition of nicotine (Figure S2) confirms that a cationic guest is required for significant binding to occur.[29] This is verified by treatment of DD1 with the quaternary ammonium ion choline at pH 12.1, for which a fluorescence response occurs (inset Fig, 1b). Sensing at various pH values will be instrumental for the simultaneous sensing of multiple analytes that have differentially charged states at the different pHs.[34-35] However, for our kinetic studies we chose the pH of 6.3 where we have the presence of only one well behaved charge state of host and guest.

The DD1-nicotine system corresponds to a system of coupled reactions requiring real-time measurement of its kinetics. The association and dissociation processes cannot be determined separately and the fastest unimolecular reaction determines the time scale for the kinetics measurements.[36] The broadening observed in the ^{1}H NMR spectra for DimerDye-guest systems,[26-27] including the current system (Figure S3), suggests that the dynamics for these systems occur on the millisecond time-scale, making stopped-flow the suitable technique for real-time kinetic measurements.[36]

The kinetics for $DD1_2$ disassembly upon dilution was measured by the appearance of fluorescence from monomeric DD1 (Figure 2b). No photoisomerization of the DD1 chromophore (HSP) occurred (Figure S4), consistent with the much slower photoisomerization for HSP observed previously.[37] At higher DD1 concentrations, the reaction is faster because of a faster rate for DD1 association to form $DD1_2$. The kinetics follow a monoexponential function from which an observed rate constant (k_{obs}) is determined. The linear dependence[38] (eq 1, see derivation in the SI) between k_{obs}^2 and the total DD1 concentration (Figure 2c) led to the determination of the association (k_a) and the dissociation (k_d) rate constants (Table 1). The ratio of k_a and k_d corresponds to the equilibrium constant for dimerization (K_{DD1}) of $(1.6 \pm 0.9) \times 10^5$ M^{-1}, a value that is similar to K_{DD1} determined from ^{1}H NMR experiments in D_2O $(3.6 \pm 0.8) \times 10^5$ M^{-1}.[26]

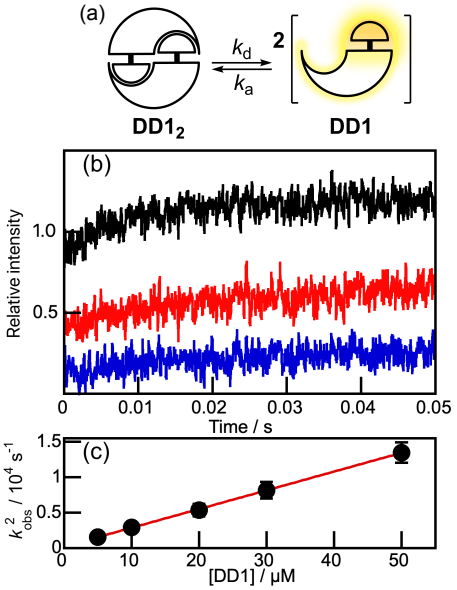

Figure 2. (a) Schematics for the dimerization of DD1. (b) Kinetics for the dilution of DD1 ($[DD1]_{final}$: blue – 5 μM, red – 10 μM, black – 50 μM) with phosphate buffer at pH 6.3. The traces are offset on the y-scale for clarity. (c) Fit to equation 1 for the dependence of k_{obs}^2 (7 independent experiments; errors correspond to standard deviations) on the DD1 concentration.

$$k_{obs}^2 = k_d^2 + 8k_a k_d[DD1]_{tot} \qquad (1)$$

Table 1. Association and dissociation rate constants for the dimerization of DD1 and the DD1-nicotine complex, and equilibrium constants for $DD1_2$ (K_{DD1}) and DDI-Nic (K_{11}) in buffer at pH 6.3 or in artificial saliva.[a]

	DD1		DD1-nicotine	
	Buffer	Saliva	Buffer	Saliva
$k_a/10^6$ M^{-1} s^{-1}	2.3±0.9	2±1		
k_d/ s^{-1}	14±6	80±40		
$K_{DD1}/10^4$ M^{-1} [b]	16±9	3±2		
$k_{11}^+/10^6$ M^{-1} s^{-1}			0.23±0.01	0.10±0.02
k_{11}^-/s^{-1}			40±10	150±30
$K_{11}/10^4$ M^{-1} [b]			0.6±0.2	0.07±0.02
$K_{11}/10^4$ M^{-1} [c]			0.6±0.1	0.13±0.02

[a]For error determinations see the Supporting Information. [b]Calculated from kinetic data, where $K_{11} = k_{11}^+ / k_{11}^-$. [c]Obtained from the binding isotherm.

The association rate constant for $DD1_2$ formation suggests that dimerization requires some rearrangement of the macrocycle to accommodate the HSP moiety, since k_a is smaller than the diffusion-controlled limit (6×10^9 M^{-1} s^{-1})[39] and smaller than the association rate constant of a neutral radical with *p*-sulfonatocalix[4]arene.[40] This moderate decrease of k_a for $DD1_2$ suggests that rearrangement and loss of entropy are required for dimerization to occur. However, no significant restrictions exist. Such restrictions, when observed for other macrocycles, like cyclodextrins and cucurbit[*n*]urils, lead to slow complexation that can take hours.[41-45] The dissociation rate constant for $DD1_2$ disassembly is similar to that for unimpeded guest dissociation from cucurbit[*n*]urils,[46-47] but much slower than the dissociation of guests from cyclodextrins.[44] This slow disassembly off-sets the low association rate constant leading to an equilibrium constant that ensures that micromolar concentrations of DD1 can be used for sensing applications.

The complexation kinetics of nicotine to DD1 do not follow a first-order behaviour because the dynamics for $DD1_2$ and DD1-nicotine occur on the same timescale (Figure 3). Global analysis was used to simultaneously fit the whole data set to a model that includes the formation of both complexes, where the values for k_a and k_d for $DD1_2$ were fixed (see SI) leading to the determination of the association (k_{11}^+) and dissociation (k_{11}^-) rate constants for DD1 complexation to nicotine (Table 1). The validity of the fitting model is evaluated from the randomness of the residuals (Figure 3b). These residuals are random at low nicotine concentrations, while the small deviations at the higher nicotine concentrations suggest the presence of minor complexes. These minor processes do not affect the accuracy of the kinetic parameters as the K_{11} values are the same when calculated from the kinetic data or from the binding isotherm obtained for the system at equilibrium (Table 1, Figure S5).

Differences in the association and dissociation rate constants for the complexation dynamics of DD1-nicotine and $DD1_2$ provide a guide for future optimization of nicotine sensing. Sensing is not optimal because with the low K_{11} for DD1-nicotine a high nicotine concentration is required to achieve detectable response. The low K_{11} compared to K_{DD1} is a consequence of the lower value of k_{11}^+ compared to k_a and the higher value of k_{11}^- compared to k_d, where the larger change for k_{11}^+ has a larger effect on K_{11}. The best target for host modification will be to increase the association rate constant k_{11}^+ in order for nicotine association to outcompete DD1 dimerization. Decreasing the nicotine dissociation rate constant would also achieve a higher K_{11} value, but too slow a nicotine dissociation rate might interfere when sensing for multiple targets is desirable.

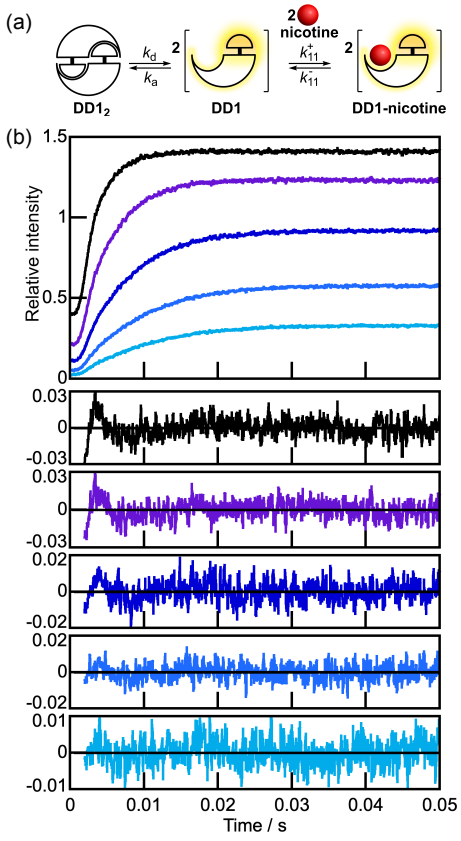

Figure 3. (a) Schematics for DD1 dimerization and nicotine binding to DD1. (b) Kinetics for the mixing of DD1 (10 μM, pH 6.3) with different concentrations of nicotine for one independent experiment. Residuals obtained for the data from the global analysis of 21 kinetic traces from four independent experiments. From the bottom to top: $[nicotine]_{final}$ = 94, 188, 375, 750 and 1500 μM.

The kinetics were also studied in artificial saliva[48] at pH 6.8 to understand how a complex environment mimicking a biological one affects the mechanism of the DD1 system. The binding affinity of nicotine to DD1 is lower (Table 1) because of the higher ionic strength of the medium, where the total cation concentration is higher than 50 mM. The kinetics for both equilibria were qualitatively the same as in buffer (Figures S6-7). The k_a for $DD1_2$ dimerization remained the same, while the rate constant for disassembly increased (Table 1). Cations are known to bind to *p*-sulfonatocalix[4]arene[49-50] and have been shown to modulate the kinetics for guest binding to a calix[6]arene in organic solvents.[51] The higher k_d for $DD1_2$ disassembly suggests that cations stabilize the monomeric DD1, while the unchanged k_a value indicates that dimerization is not inhibited by cation binding to DD1, ensuring that the decrease of K_{DD1} is only modest. The trends for the dynamics of DD1-nicotine were the same as in buffer with a further decrease observed for k_{11}^+ and a more significant increase observed for k_{11}^-. From the mechanistic point of view the relative rate constant for $DD1_2$ dimerization

and DD1-nicotine complexation did not change significantly, showing that mechanistic kinetic studies in buffer provide relevant information for the design of the next generation of disassembly driven sensors.

In the context of systems chemistry, the two competing equilibria characterized in this paper are on the simpler end of the complexity spectrum. And yet, the kinetic studies of this 'simple' system reveal striking complexity in the coupling of the two equilibria, in their generation of optical outputs, and in their strong dependence on pH and co-solutes. The quest for emergent properties is one of the main motivations for doing systems chemistry, and yet we often do not know how to tune those properties. This study shows how kinetic information provides means for the rational tuning of the responses of host-guest systems that could lead to the emergence of improved functions in a family of supramolecular sensors.

EXPERIMENTAL SECTION

Materials. DD1 was synthesized and purified following the reported protocols and the purity was verified by UPLC-MS (Figure S8).[26] Guest compounds (S)-(-)-nicotine (99%) and choline chloride (>98%) did not show any fluorescent impurities. The artificial saliva materials were: methyl 4-hydroxybenzonate, sodium carboxymethyl cellulose, potassium chloride, calcium chloride, potassium dihydrogen phosphate, and magnesium chloride. Dibasic sodium phosphate, monobasic sodium phosphate, potassium hydroxide, sodium hydroxide and hydrochloric acid were used without further purification.

Sample preparation. All solutions, with the exception of the ones for ^{1}H NMR experiments, were prepared using deionized water (Barnstead NANOpure deionizing systems, ≥17.8 MΩ cm). The pH values were confirmed using a Cole Parmer Microcomputer pH-Vision pH meter. For ^{1}H NMR experiments, the solutions were prepared using NaH_2PO_4/Na_2HPO_4 (50 mM, pD 6.3) in D_2O. For all other studies, phosphate buffer (10 mM, pH 6.3) was prepared using NaH_2PO_4/Na_2HPO_4 in deionized water. The pH was adjusted with 1 M NaOH/HCl. HCl solutions of pH 2.2 and NaOH solutions of pH 12.1 were prepared from a 4.0 N HCl stock solution and solid NaOH, respectively. Artificial saliva (pH 6.8) was prepared following the reported protocol.[48] The concentrations of the artificial saliva components are: [methyl 4-hydroxybenzonate] = 13 mM, [sodium carboxymethyl cellulose] = 38 mM, [KCl] = 8.4 mM, [$CaCl_2$] = 1.5 mM, [KH_2PO_4] = 2.4 mM and [$MgCl_2$] = 0.6 mM. The pH was adjusted using 1 M KOH and the solution was then filtered. Solutions of DD1 and nicotine were made in the phosphate buffer (10 mM, pH 6.3), hydrochloric acid (10 mM, pH 2.2), NaOH (10 mM, pH 12.1) and artificial saliva (pH 6.8) solutions. A stock solution of choline chloride was made in NaOH (10 mM, pH 12.1). These stocks were further diluted with the corresponding buffer, acid, base, or saliva solution to afford the concentrations specified in the UV-Vis absorption, steady-state fluorescence and stopped-flow experiments. During stopped-flow experiments the concentrations of the solutions are halved due to equal volume mixing of the two solutions placed in each syringe before the measurement. For binding isotherm measurements, the nicotine solution contained the same concentration of DD1 as the DD1solution into which nicotine was titrated into, so that dilution of DD1 did not occur during the experiment.

Equipment. The ^{1}H NMR spectra were recorded on a Bruker Avance Neo 500 MHz spectrometer at 24°C. The UV-Vis absorption spectra were recorded on a Varian Cary 100 spectrophotometer. Fluorescence emission spectra were collected using a PTI QM40 fluorimeter. In the case of the DD1-nicotine system, the steady-state fluorescence emission was collected from 400-700 nm at an excitation wavelength of 375 nm. The excitation and emission monochromator bandwidths were set to 2 nm for all these measurements. For the binding isotherm experiments at pH 6.3, the emission spectra were collected between 400 and 700 nm at an excitation wavelength of 384 nm.

An Applied Photophysics SX20 stopped-flow spectrometer, with a Hg-Xe vapour lamp as the excitation source, was used to measure the homodimerization and binding dynamics in phosphate buffer and artificial saliva. Two solutions were mixed within ~ 1 ms in a 1:1 ratio. For the homodimerization and binding dynamics studies in the presence of phosphate buffer or artificial saliva, the samples were excited at 400 and 405 nm respectively, with an excitation monochromator slit width of 2 mm that corresponds to a bandwidth of 9.3 nm. The emission from the sample was collected using a 515 nm cut-off filter. The sample temperatures were maintained at 20ºC using a water bath.

ASSOCIATED CONTENT

Supporting Information

The Supporting Information is available free of charge on the ACS Publications website.

Absorption and fluorescence spectra at different pH values, ^{1}H NMR spectra for DD1 and DD1-nicotine, DD1 photostability studies, global analysis on the DD1-nicotine kinetics, binding isotherm for DD1-nicotine, kinetics for DD1-nicotine in artificial saliva, and UPLC-MS DD1 experiment.

AUTHOR INFORMATION

Corresponding Author

Fraser Hof – Department of Chemistry and Centre for Advanced Materials and Related Technologies (CAMTEC), University of Victoria, Victoria, BC V8W 2Y2, Canada; Email: fhof@uvic.ca.

Cornelia Bohne – Department of Chemistry and Centre for Advanced Materials and Related Technologies (CAMTEC), University of Victoria, Victoria, BC V8W 2Y2, Canada; Email: cornelia.bohne@gmail.com.

Author Contributions

Cara Gallo: Investigation, formal data analysis. Suma S. Thomas: Formal analysis, supervision, writing, visualization. Allison J. Selinger: Supervision, writing, visualization. Fraser Hof: Conceptualization, writing, review and editing. Cornelia Bohne: Conceptualization, writing, review and editing.

Notes

The authors declare no competing financial interest.

ACKNOWLEDGMENT

The authors thank the Natural Sciences and Engineering Research Council of Canada (NSERC) for financial support (CB-RGPIN-2017-04458; FH-RGPIN-2019-04806) and CAMTEC for the use of shared facilities.

REFERENCES

1. Sedwick, A. C.; Brewster II, J. T.; Wu, T.; Feng, X.; Bull, S. D.; Qian, X.; Sessler, J. L.; T.D., J.; Anslyn, E. V.; Sun, X., Indicator

displacement assays (IDAs): the past, present and future. *Chem. Soc. Rev.* **2021,** *50*, 9-38.

2. Guo, C.; Sedwick, A. C.; T., H.; Sessler, J. L., Supramolecular fluorescent sensors: An historical overview and update. *Coord. Chem. Rev.* **2021,** *427*, 213560.

3. Pinalli, R.; Pedrini, A.; Dalcanale, R., Biochemical sensing with macrocyclic receptors. *Chem. Soc. Rev.* **2018,** *47*, 7006-7026.

4. Kumar, R.; Sharma, A.; Singh, H.; Suating, P.; Kim, H. S.; Sumwoo, K.; Shim, I.; Gibb, B. C.; Kim, J. S., Revisiting Fluorescent Calixarenes: From Molecular Sensors to Smart Materials. *Chem. Rev.* **2019,** *119*, 9657-9721.

5. Ghale, G.; Nau, W. M., Dynamically Analyte-Responsive Macrocyclic Host−Fluorophore Systems. *Acc. Chem. Res.* **2014,** *47*, 2150-2159.

6. Mizusawa, K.; Ishida, Y.; Takaoka, Y.; Miyagawa, M.; Tsukiji, S.; Hamachi, I., Disassembly-Driven Turn-On Fluorescent Nanoprobes for Selective Protein Detection. *J. Am. Chem Soc.* **2010,** *132*, 7291-7293.

7. Bo, F.; Gao, B.; Duan, W.; Li, H.; Liu, H.; Bai, Q., Assembly–disassembly driven ''off–on'' fluorescent perylene bisimide probes for detecting and tracking of proteins in living cells. *RSC Adv.* **2013,** *3*, 17007-17010.

8. Tian, D.; Li, F.; Zhu, Z.; Zhang, L.; Zhu, J., An AIE-based metallo-supramolecular assembly enabling an indicator displacement assay inside living cells. *Chem. Commun.* **2018,** *54*, 8921-8924.

9. Sakai, R.; Nagai, A.; Tago, Y.; Sato, S.; Arai, T.; Satoh, T.; Kakuchi, T., Fluorescence Turn-On Sensing of Anions Based on Disassembly Process of Urea-Functionalized Poly(phenylenebutadiynylene) Aggregates. *Macromolecules* **2012,** *45*, 4123-4127.

10. Savariar, E. N.; Ghosh, S.; González, D. C.; Thayumanavan, S., Disassembly of Noncovalent Amphiphilic Polymers with Proteins and Utility in Pattern Sensing. *J. Am. Chem Soc.* **2008,** *130*, 5416-5417.

11. González, D. C.; Savariar, E. N.; Thayumanavan, S., Fluorescence Patterns from Supramolecular Polymer Assembly and Disassembly for Sensing Metallo- and Nonmetalloproteins. *J. Am. Chem Soc.* **2009,** *131*, 7708-7716.

12. Azagarsamy, M. A.; Yesilyurt, V.; Thayumanavan, S., Disassembly of Dendritic Micellar Containers Due to Protein Binding. *J. Am. Chem Soc.* **2010,** *132*, 4550-4551.

13. Tanwar, A. S.; Yver, P. K., Fluorescence "Turn-On" Indicator Displacement Assay-Based Sensing of Nitroexplosive 2,4,6-Trinitrophenol in Aqueous Media via a Polyelectrolyte and Dye Complex. *ACS Omega* **2017,** *2*, 4424-4430.

14. Liu, Y.; Perez, L.; Mettry, M.; Easley, C. J.; Hooley, R. J.; Zhong, W., Self-Aggregating Deep Cavitand Acts as a Fluorescence Displacement Sensor for Lysine Methylation. *J. Am. Chem Soc.* **2016,** *138*, 10746-10749.

15. Gill, A. D.; Hickey, B. L.; Zhong, W.; Hooley, R. J., Selective sensing of THC and related metabolites in biofluids by host:guest arrays. *Chem. Commun.* **2020,** *56*, 4352-4355.

16. Gill, A. D.; Perez, L.; Salinas, I. N. Q.; Byers, S. R.; Liu, Y.; Hickey, B. L.; Zhong, W.; Hooley, R. J., Selective Array-Based Sensing of Anabolic Steroids in Aqueous Solution by Host–Guest Reporter Complexes. *Chem. Eur. J.* **2019,** *25*, 1740-1745.

17. Liu, Y.; Perez, L.; Gill, A. D.; Hooley, R. J.; Zhong, W., Selective Sensing of Phosphorylated Peptides and Monitoring Kinase and Phosphatase Activity with a Supramolecular Tandem Assay. *J. Am. Chem Soc.* **2018,** *140*, 13869-13877.

18. Liu, Y.; Perez, L.; Mettry, M.; Gill, A. D.; Byers, S. R.; Easley, C. J.; Bardeen, C. J.; Zhong, W.; Hooley, R. J., Site selective reading of epigenetic markers by a dual-mode synthetic receptor array. *Chem. Sci.* **2017,** *8*, 3960-3970.

19. Gill, A. D.; Hickey, B. L.; Wang, S.; Xue, M.; Zhong, W.; Hooley, R. J., Sensing of citrulline modifications in histone peptides by deep cavitand hosts. *Chem. Commun.* **2019,** *55*, 13259-13262.

20. Ashkenasy, G.; Hermans, T. M.; Otto, S.; Taylor, A. F., Systems Chemistry. *Chem. Soc. Rev.* **2017,** *46*, 2543-2554.

21. Mattia, E.; Otto, S., Supramolecular systems chemistry. *Nat. Nanotechnol.* **2015,** *10*, 111-119.

22. Thomas, S. S.; Tang, H.; Bohne, C., Noninnocent Role of Na^+ Ions in the Binding of the N-Phenyl-2-naphthylammonium Cation as a Ditopic Guest with Cucurbit[7]uril. *J. Am. Chem Soc.* **2019,** *141*, 9645-9654.

23. Florea, M.; Kudithipudi, S.; Rei, A.; González-Álvarez, M. J.; Jeltsch, A.; Nau, W. M., A Fluorescence-Based Supramolecular Tandem Assay for Monitoring Lysine Methyltransferase Activity in Homogeneous Solution. *Chem. Eur. J.* **2012,** *18*, 3521-3528.

24. Yesilyurt, V.; Ramireddy, R.; Azargarsamy, M. A.; Thayumanavan, S., Accessing Lipophilic Ligands in Dendrimer-Based Amphiphilic Supramolecular Assemblies for Protein-Induced Disassembly. *Chem. Eur. J.* **2012,** *18*, 223-229.

25. Beatty, M. A.; Busmann, J. A.; Fagen, N. G.; Garnett, G. A. E.; Hof, F., A clip-like host that undergoes self-assembly and competitive guest-induced disassembly in water. *Supramol. Chem.* **2019,** *31*, 101-107.

26. Beatty, M. A.; Borges-González, J.; Sinclair, N. J.; Pye, A. T.; Hof, F., Analyte-Driven Disassembly and Turn-On Fluorescent Sensing in Competitive Biological Media. *J. Am. Chem. Soc.* **2018,** *140*, 3500-3504.

27. Beatty, M. A.; Selinger, A. J.; Hof, F., Parallel Synthesis and Screening of Supramolecular Chemosensors That Achieve Fluorescent Turn-on Detection of Drugs in Saliva. *J. Am. Chem Soc.* **2019,** *141*, 16763-16771.

28. Beatty, M. A.; Pye, A. T.; Kim, B.; Selinger, A. J.; Hof, F., Using reversible non-covalent and covalent bonds to create assemblies and equilibrating molecular networks that survive 5 molar urea. *Org, Biomol. Chem.* **2019,** *17*, 2081-2086.

29. Warmerdam, Z.; Kamba, B. E.; Saurya, A.; Sun, X.; Maguire, M. K.; Hof, F., Calix[4]arene sulfonate hosts selectively modified on the upper rim: a study of nicotine binding strength and geometry. *in press* **2021,** *https://doi.org/10.1080/10610278.2021.1873991*.

30. El-Hellani, A.; El-Hage, R.; Baalbaki, R.; Salman, R.; Talih, S.; Shihadeh, A.; Saliba, N. A., Free-Base and Protonated Nicotine in Electronic Cigarette Liquids and Aerosols. *Chem. Res. Toxicol.* **2015,** *28*, 1532-1537.

31. Gallo, C.; Thomas, S. S.; Selinger, A. J.; Hof, F., Mechanism of a Disassembly Driven Sensing System Studied by Stopped-Flow Kinetics. *ChemRxiv*, April 15, 2021, https://doi.org/10.26434/chemrxiv.14410775.v1.

32. Yoshida, I.; Yamamotu, N.; Fumio, S.; Ishii, D.; Ueno, K.; Shinkai, S., Re-evaluation of the Acid Dissociation Constants of the Hydroxyl Groups in Tetrasodium 25,26,27,28-Tetrahydroxycalix[4]arene-5,11,17,23-tetrasulfonate *Bull. Chem. Soc. Jpn.* **1992,** *65*, 1012-1015.

33. Hajmalek, M.; Kalili, M. S.; Zare, K.; Zabihi, O., Determination of the acid dissociation constants of the p-sulphonato-calix[4]arene. *J. Nanoanalysis* **2014,** *1*, 47-51.

34. Liu, Y.; Perez, L.; Gill, A. D.; Mettry, M.; L., L.; Wang, Y.; Hooley, R. J.; Zhong, W., Site-Selective Sensing of Histone Methylation Enzyme Activity via an Arrayed Supramolecular Tandem Assay. *J. Am. Chem Soc.* **2017,** *139*, 10964-10967.

35. Minaker, S. A.; Daze, K. D.; Ma, M. C. F.; Hof, F., Antibody-Free Reading of the Histone Code Using a Simple Chemical Sensor Array. *J. Am. Chem Soc.* **2012,** *134*, 11674-11680.

36. Bohne, C., Supramolecular Dynamics. *Chem. Soc. Rev.* **2014,** *43*, 4037-4050.

37. Tang, H.; Thomas, S. S.; Wolf, L.; Natarajan, P.; Ko, Y. H.; Wilson, J.; Kim, K.; Bohne, C., Nonlinear Dependence on Na^+ Ions for the Binding Dynamics of Cucurbit[6]uril with the trans-1-Methyl-4-(4-hydroxystyryl)pyridinium Cation. *J. Phys. Chem. B* **2020,** *124* (45), 10219-10225.

38. Bernasconi, C. F., *Relaxation Kinetics*. Academic Press, Inc.: New York, 1976; p 288.

39. Montalti, M.; Credi, A.; Prodi, L.; Gandolfi, M. T., *Handbook of Photochemistry*. 3rd ed.; CRC Press: Boca Raton, 2006.

40. Franchi; Lucarini, M.; Pedulli, G. F.; Sciotto, D., An EPR Investigation of the Kinetics of Inclusion of a Persistent Radical in Water-Soluble Calix[4]arenes. *Angew. Chem. Int. Ed.* **2000,** *39*, 263-266.

41. Cramer, F.; Saenger, W.; Spatz, H.-C., Inclusion Compounds. XIX. The Formation of Inclusion Compounds of a-Cyclodextrin in Aqueous Solutions. Thermodynamics and Kinetics. *J. Am. Chem. Soc.* **1967,** *89*, 14-20.

42. Mock, W. L.; Shih, N. Y., Structure and selectivity in host-guest complexes of cucurbituril. *J. Org. Chem.* **1986,** *51* (23), 4440-4446.

43. Marquez, C.; Nau, W. M., Two Mechanisms of Slow Host-Guest Complexation Between Cucurbit[6]uril and Cyclohexylmethylamine: pH-Responsive Supramolecular Kinetics. *Angew. Chem. Int. Ed.* **2001,** *40* (17), 3155-3160.

44. Bohne, C., Supramolecular Dynamics Studied Using Photophysics. *Langmuir* **2006,** *22*, 9100-9111.

45. Masson, E.; Raeisi, M.; Kotturi, K., Kinetics Inside, Outside and Through Cucurbiturils. *Isr. J. Chem.* **2018,** *58* (3-4), 413-434.

46. Tang, H.; Fuentealba, D.; Ko, Y. H.; Selvapalam, N.; Kim, K.; Bohne, C., Guest Binding Dynamics with Cucurbit[7]uril in the Presence of Cations. *J. Am. Chem. Soc.* **2011,** *133*, 20623-20633.

47. Thomas, S. S.; Bohne, C., Determination of the kinetics underlying the pK_a shift for the 2-aminoanthracenium cation binding with cucurbit[7]uril. *Faraday Discuss.* **2015,** *185*, 381-398.

48. Alshali, R. Z.; Salim, N. A.; Satterthwaite, J. D.; Silikas, N., Long-term Sorption and Solubility of Bulk-fill and Conventional Resin-composites in Water and Arificial Saliva. *J. Dent.* **2015,** *43*, 1511-1518.

49. Basilio, N.; García-Río, L.; Martín-Pastor, M., Counterion Binding in Solutions of p-Sulfonatocalix[4]arene. *J. Phys. Chem. B* **2010,** *114*, 7201-7206.

50. Francisco, V.; Piñero, A.; Nau, W. M.; García-Río, L., The "True" Affinities of Metal Cations to p-Sulfonatocalix[4]arene: A Thermodynamic Study at Neutral pH Reveals a Pitfall Due to Salt Effects in Microcalorimetry. *Chem. Eur. J.* **2013,** *19*, 17809-12820.

51. Credi, A.; Dumas, S.; Silvi, S.; Venturi, M.; Arduini, A.; Pochini, A.; Secchi, A., Viologen-Calix[6]arene Pseudorotaxanes. Ion-Pair Recognition and Threading/Dethreading Molecular Motions. *J. Org. Chem.* **2004,** *69*, 5881-5887.